ResearchGate

See discussions, stats, and author profiles for this publication at: https://www.researchgate.net/publication/268557766

Nonlinear Dynamic Inversion and Block Backstepping: A Comparison

Conference Paper · August 2012

DOI: 10.2514/6.2012-4888

CITATIONS
7

READS
157

3 authors, including:

Fredrik Berefelt
Swedish Defence Research Agency
4 PUBLICATIONS **23** CITATIONS

SEE PROFILE

All content following this page was uploaded by Fredrik Berefelt on 18 September 2018.

The user has requested enhancement of the downloaded file.

AIAA Guidance, Navigation, and Control Conference
13 - 16 August 2012, Minneapolis, Minnesota

AIAA 2012-4888

Nonlinear Dynamic Inversion and Block Backstepping: A Comparison

Johan Knöös*, John W.C. Robinson†, and Fredrik Berefelt‡

Nonlinear dynamic inversion by time scale separation (NDI) offers a quick and simple design route for (full three axis) nonlinear flight control law design that yields a low complexity control law. The resulting closed loop system can be made semiglobally stable but the stability is critically dependent on the fulfillment of the time scale separation assumption which in general forces the inner loop (angular rates) to be considerably faster than the outer loop (velocity components). Block backstepping (BBS) is an alternative design method that does not rely on a time scale separation requirement and directly yields semiglobal stability but that involves a somewhat more complicated design procedure and resulting control law. The two methods are closely related, however, and in this paper we make a comparison of them. In particular, we show conditions under which the extra terms in the BBS control law offer (or do not offer) significant advantages over the simple NDI control law. We show this in terms of stability region, sensitivity, and robustness.

I. Introduction

Nonlinear design methods for flight control law design are by now an established alternative to the classic and modern linear methods. The two main drivers for employing nonlinear techniques are the possibility of achieving better performing controllers, especially for highly maneuverable aircraft, and the ability to reduce design cycle time by avoiding gain scheduling and the associated tuning process.[1] Some of the most popular nonlinear approaches (for full three axis control) are feedback linearization[2] (exact linearization), (block) backstepping,[3] and nonlinear dynamic inversion via time scale separation.[4] The latter is an approximation to feedback linearization where the idea[5] is to locate variables that are slow compared to others and neglect these in certain time differentiations (or the corresponding Lie derivative components) thereby breaking the design into two independent problems (loops). In this work we deal exclusively with the version of nonlinear dynamic inversion that works by time scale separation, abbreviated NDI, and compare it to block backstepping, abbreviated BBS.

The fact that NDI relies on a time scale separation assumption makes stability issues even more delicate than feedback linearization (which, in theory, requires an exact model of the plant and only guarantees local asymptotic stability). This issue was realized early and motivated several robustness studies.[6,7,8,5] Backstepping, on the other hand, does not rely on a time scale separation assumption, yields semiglobal stability, and is not inherently non-robust. Moreover, it can easily be modified to explicitly handle so called matched disturbances (disturbance terms "reachable" by a control or virtual control).[9] A possible drawback with the backstepping control approach compared to the NDI approach, however, is that it results in a more complex control law. This forces the designer to weigh the low complexity and easily understood mechanics of the NDI control law against the more complex and perhaps less intuitive backstepping control law, where it is not fully transparent what the effect of the different terms are on the closed loop system properties.

In this work we address these trade-off issues and investigate the relative merits of block backstepping BBS versus NDI from different angles. In particular, we study the relation between time scale separation and stability for NDI and how time scale separation affects performance for BBS. We also consider the classical

*Student, Royal Institute of Technology (KTH), School of Engineering Sciences, 100 44, Stockholm, Sweden, AIAA student member.

†Deputy Research Director, Department of Aeronautics, Swedish Defence Research Establishment (FOI), 164 90, Stockholm, Sweden, AIAA member.

‡Senior Scientist, Department of Aeronautics, Swedish Defence Research Establishment (FOI), 164 90, Stockholm, Sweden, AIAA member.

Copyright © 2012 by Johan Knöös, John W.C. Robinson, Fredrik Berefelt. Published by the American Institute of Aeronautics and Astronautics, Inc., with permission.

sensitivity function properties of both methods and show how the greater degrees of design freedom for BBS can be used to balance the trade-off issues for the designer. To a large extent we employ linear analysis methods for the closed loop system since we believe that a great deal of insight about these issues in flight mechanical applications can be gained from studying the linearized (closed loop) systems.

The outline of the paper is as follows. In the next section we introduce a generic model for six degrees of freedom flight mechanics that we later use as template when describing and analyzing the BBS and NDI methods. We then review the sensitivity and time scale separation measures we use and illustrate some of the effects related to time scale separation and stability with a simple pitch plane model. After this we investigate differences in performance for BBS and NDI numerically using a reusable launch vehicle (RLV) as an example. Finally, we summarize the results and offer some conclusions that can be drawn from these.

NOTATION. Vectors and matrices are marked with ordinary font, with lower case letters indicating vectors and upper case indicating matrices. The transpose of a vector or matrix is denoted as x^T. The set of eigenvalues (spectrum) of a matrix square A is marked as $\lambda(A)$. The largest and smallest eigenvalues of a square matrix A with a real spectrum are denoted $\lambda_{\max}(A)$ and $\lambda_{\min}(A)$, respectively. A square matrix with all its spectrum contained in the open left half-plane of the complex plane is said to be Hurwitz. The Jacobian matrix of a vector valued smooth function f is denoted $\partial f(x)/\partial x$. Time derivatives are marked with a dot like $\dot{x}$. The identity matrix is marked as I, where the dimension is marked with a subscript, e.g. I_3, when needed, and similarly for a square zero matrix. For a moment of inertia matrix we use the symbol J.

II. Model and Control Problem

We shall here introduce a flight mechanical model which is adapted to our application example. Most of what follows, however, is generic for many flight control applications and is not critically dependent on the formulation (e.g. choice of state variables) used here.

II.A. Six degrees of freedom aircraft dynamics

The central part of most flight mechanical models are the Newton-Euler (N-E) equations for rigid body motion expressed in the body frame

$$\begin{aligned} \dot{v}^{(b)} &= \frac{1}{m} f^{(b)} + v^{(b)} \times \omega^{(b)}, \\ \dot{\omega}^{(b)} &= J^{-1} m^{(b)} - J^{-1}(\omega^{(b)} \times J\omega^{(b)}), \end{aligned} \tag{1}$$

where $v^{(b)}, \omega^{(b)} \in \mathbb{R}^3$ are the velocity and angular rate vectors in the body frame, m is the total mass, $J \in \mathbb{R}^{3\times 3}$ is the matrix of inertia in the body frame around the center of mass (CoM), and $f^{(b)}, m^{(b)} \in \mathbb{R}^3$ are the forces and moments (around CoM), respectively. Effects of gravity, thrust (whenever present), and air density enter into $f^{(b)}, m^{(b)}$ and since these effects depend on additional variables such as altitude and the relative orientation between the body frame and Earth, additional equations are in general added to the N-E system. For the control applications we are using to illustrate the theory, control of a reusable launch vehicle in atmospheric descent, the most important additional variables are the Euler bank angle ϕ and Euler pitch angle θ. We shall assume that airspeed $V = \|v^{(b)}\|$ varies slowly compared to the angle of attack α, sideslip angle β, and bank angle ϕ, and that the Euler pitch angle θ is small at all times. Therefore, we shall neglect the effect of θ and take V as constant in our dynamics formulation. Moreover, we shall make the important assumption that the control surface deflections produce forces that are negligible[a] in $f^{(b)}$. In addition, we assume that $f^{(b)}$ is independent of the angular rates $\omega^{(b)}$. Under these assumptions it is reasonable to consider the dynamics for $\psi \in \mathbb{R}^6$ given by

$$\psi = \begin{bmatrix} \chi \\ \omega^{(b)} \end{bmatrix}$$

where $\chi \in \mathbb{R}^3$ is given by

$$\chi = [\alpha, \beta, \phi]^T.$$

[a]This is often not entirely realistic but is needed for application of the control methods considered here. Moreover, the effect of this assumption can to some extent be investigated with the robustness tool discussed in later sections.

The dynamics for χ can, assuming $\theta = 0$, be written on the form (see [10, Sec. 2.5])

$$\dot{\chi} = \frac{1}{mV}\begin{bmatrix} -\sin\alpha/\cos\beta & 0 & \cos\alpha/\cos\beta \\ -\cos\alpha\sin\beta & \cos\beta & -\sin\alpha\sin\beta \\ 0 & 0 & 0 \end{bmatrix} f^{(b)}(\chi) + \begin{bmatrix} -\cos\alpha\tan\beta & 1 & -\sin\alpha\tan\beta \\ \sin\alpha & 0 & -\cos\alpha \\ 1 & 0 & 0 \end{bmatrix} \omega^{(b)}, \quad (2)$$

where all dependence in $f^{(b)}$ of the auxiliary variables has been suppressed.

II.B. Open loop dynamics

In view of the above we shall formulate our control problems for a generic plant model of the form

$$\dot{x} = f(x) + G(x)\omega, \quad (3)$$

$$\dot{\omega} = h(x,\omega) + Ku, \quad (4)$$

defined for (x,ω) in a bounded open subset $\mathcal{D} = \mathcal{D}_x \times \mathcal{D}_\omega \subseteq \mathbb{R}^3 \times \mathbb{R}^3$ including the origin (in the interior of $\mathcal{D}$). The (time varying) vector u is a "generic" control signal (which can be taken to be control surface deflections, assuming linear effect of these, or moments since control surface moments and forces are bijectively related in most parts of the envelope). It is assumed that for $u = 0$ the point $(x,\omega) = (0,0)$ is an equilibrium point for the system in Eqs. (3) and (4) (which implies $f(0) = 0$ and $h(0,0) = 0$). It is further assumed that the vector fields f, h are C^1, that the constant matrix $K \in \mathbb{R}^{3\times3}$ is invertible and that the matrix $G \in \mathbb{R}^{3\times3}$ of (columnwise) vector fields is continuous and has a continuous inverse on the closure of $\mathcal{D}$. The latter in particular implies that G^{-1} is bounded on $\mathcal{D}$. It is easy to add extra integrator states[11,12] to x, e.g. in order to be able to synthesize second order dynamics for the desired dynamics in the x-system or just to add integral action. However, to keep the presentation simple, we shall only consider the first order case here.

The formulation in Eqs. (3) and (4) does not contain any reference signals (to dictate the physical reference point which should define an equilibrium (trim) point for the dynamic system). Absence of explicit reference signals in Eqs. (3) and (4) is equivalent to only considering constant reference signals since for such reference signals the system can always, after a (time invariant) change of variables, be brought back to the form in Eqs. (3) and (4). Introducing time varying reference signals, which is equivalent to going to a tracking formulation, would lead to a time varying system. However, since the only time varying terms would be the time derivatives of the reference signals it is easy to adapt many of the results, in particular the Lyapunov stability arguments, also to this time varying situation (cf. e.g. Refs. 11, 13). For this reason, and for the reason that many powerful linear techniques are restricted to the time invariant case, we shall here only consider set point control formulations based on Eqs. (3) and (4).

II.C. Error system

In both block backstepping and nonlinear dynamic inversion the concept of a virtual control law enters (and is in fact central). A *virtual control law* $\mu : \mathcal{D}_x \to \mathbb{R}^3$ is here a function of the velocity states such that

$$f(x) + G(x)\mu(x) = f_d(x), \quad (5)$$

where f_d is a vector field with $f_d(0) = 0$ that yields some desired or nominal dynamics for the x-subsystem

$$\dot{x} = f_d(x). \quad (6)$$

The function μ is prescribed to be at least continuously differentiable on $\mathcal{D}$ and to vanish at the origin, viz.

$$\mu(0) = 0. \quad (7)$$

For later use we note that by the assumptions on G we can explicitly solve for μ from Eq. (5) as

$$\mu(x) = G^{-1}(x)\left(f_d(x) - f(x)\right). \quad (8)$$

The property of Eq. (7) makes it possible to make a change of variables and replace Eq. (4) with an error equation based on the error variable

$$z = \omega - \mu(x). \quad (9)$$

In terms of the error variable z and the desired dynamic f_d Eq. (3) can equivalently be written

$$\dot{x} = f_d(x) + G(x)z. \tag{10}$$

The (open loop) dynamics for z are given by

$$\begin{aligned}\dot{z} &= h(x, z+\mu(x)) + Ku - \frac{\partial \mu(x)}{\partial x}\left(f(x) + G(x)(z+\mu(x))\right) \\ &= \tilde{h}(x,z) + Ku - \frac{\partial \mu(x)}{\partial x}\left(f_d(x) + G(x)z\right)\end{aligned} \tag{11}$$

where

$$\tilde{h}(x,z) = h(x, z+\mu(x)).$$

With the property of Eq. (7), the point $(x,\omega) = (0,0)$ is an equilibrium point for $u = 0$ to the system in Eqs. (3) and (4) if and only if $(x,z) = (0,0)$ is an equilibrium point for $u = 0$ to the system in Eqs. (10) and (11). In discussions of the open loop (nonlinear) dynamics we shall henceforth almost exclusively consider the system in Eqs. (10) and (11). The closed loop versions of Eqs. (10) and (11) will be referred to as the *slow system/loop* and *fast system/loop*, respectively.

II.D. Linearized error system

If we introduce

$$A = \left.\frac{\partial f(x)}{\partial x}\right|_{x=0}, \quad A_d = \left.\frac{\partial f_d(x)}{\partial x}\right|_{x=0}, \quad G = G(0), \tag{12}$$

we see from Eq. (8) that the linearization $\tilde{\mu}$ of the virtual control law μ around 0 is given by

$$\tilde{\mu}(x) = G^{-1}(A_d - A)x.$$

It follows that the linearization around $(x,z) = (0,0)$ of Eqs. (10) and (11) is

$$\dot{x} = A_d x + Gz, \tag{13}$$

$$\dot{z} = Ex + Fz + Ku - G^{-1}(A_d - A)(A_d x + Gz), \tag{14}$$

where

$$F = \left.\frac{\partial \tilde{h}(x,z)}{\partial z}\right|_{(x,z)=(0,0)} = \left.\frac{\partial h(x,z)}{\partial z}\right|_{(x,z)=(0,0)}, \tag{15}$$

$$\begin{aligned}E = \left.\frac{\partial \tilde{h}(x,z)}{\partial x}\right|_{(x,z)=(0,0)} &= \left.\frac{\partial h(x,z)}{\partial x}\right|_{(x,z)=(0,0)} + \left.\frac{\partial h(x,z)}{\partial z}\right|_{(x,z)=(0,0)} \left.\frac{d\mu(x)}{dx}\right|_{x=0} \\ &= \left.\frac{\partial h(x,z)}{\partial x}\right|_{(x,z)=(0,0)} + FG^{-1}(A_d - A).\end{aligned} \tag{16}$$

In order to conform with subsequent stability analysis requirements we shall henceforth assume that A_d is Hurwitz.

II.D.1. State space form

The linearized error system in Eqs. (13) and (14) can be written more compactly as

$$\dot{\xi} = A_e \xi + B_e u \tag{17}$$

where the state $\xi \in \mathbb{R}^6$, system matrix $A_e \in \mathbb{R}^{6\times 6}$, and control gain matrix $B_e \in \mathbb{R}^{6\times 3}$ are given by

$$\xi = \begin{bmatrix} x \\ z \end{bmatrix}, \quad A_e = \begin{bmatrix} A_d & G \\ E - G^{-1}(A_d - A)A_d & F - G^{-1}(A_d - A)G \end{bmatrix}, \quad B_e = \begin{bmatrix} 0_3 \\ K \end{bmatrix}.$$

II.E. Transfer function representation of the open loop system

The transfer function (matrix, operator) P from u to $\xi = (x, z)$ for the linearized open loop error system in Eqs. (13)–(17) is a matrix with values in $\mathbb{C}^{6\times 3}$ given by

$$P(s) = (sI_6 - A_e)^{-1}B_e. \tag{18}$$

Different forms of output functions for this system can be obtained by defining and applying a "selection" matrix $M \in \mathbb{R}^{3\times 6}$ to the state. We shall only consider the two cases $M = M_1$ and $M = M_2$ where

$$M_1 = \begin{bmatrix} I_3 & 0_3 \end{bmatrix} \quad \text{and} \quad M_2 = \begin{bmatrix} 0_3 & I_3 \end{bmatrix}, \tag{19}$$

and we shall concentrate on the latter case. Likewise we shall consider a disturbance signal n with values in $\mathbb{R}^3$ acting on "either half" the state vector, i.e. we shall consider the product Nn acting on the state vector where $N \in \mathbb{R}^{6\times 3}$ the "distribution" matrix defining the input function. We shall only consider the two cases $N = N_1$ and $N = N_2$ where

$$N_1 = \begin{bmatrix} I_3 \\ 0_3 \end{bmatrix} \quad \text{and} \quad N_2 = \begin{bmatrix} 0_3 \\ I_3 \end{bmatrix}. \tag{20}$$

III. Block Backstepping and Nonlinear Dynamic Inversion

We shall now describe the BBS and NDI control laws. The two control laws are related, but the BBS control law contains (three) extra terms compared to the NDI law and in the later sections we show the function and merit of these terms.

III.A. Block backstepping

The block backstepping design is a recursive Lyapunov design[14] in which a stabilizing control ν and Lyapunov function V are constructed simultaneously. The control ν is of (static) state feedback type (using the entire state vector (x, ω), expressed in terms of the pair (x, z)).

III.A.1. Design procedure

Step 1. The first step in the BBS design is to define a virtual control law μ as in Eqs. (5) and (6) for which a Lyapunov function V_1 is known.[b] The Lyapunov function V_1 selected in the first step is normally of the simple quadratic form

$$V_1(x) = \frac{1}{2}x^T Q_x x, \tag{21}$$

where Q_x is a square symmetric positive definite matrix. Using V_1 in Eq. (21) as a start, a Lyapunov function for the entire (x, z)-system is then constructed. If further ("higher order derivative"-) subsystems are present (e.g. actuator dynamics), the procedure can be repeated in a recursive fashion.

Step 2. In this step one or several additional terms are added to V_1 in order to form a Lyapunov function (candidate) for the overall system in Eqs. (10) and (11). In the simplest case a single term of the form

$$V_2(z) = \frac{1}{2}z^T Q_z z$$

is added, where Q_z is a square symmetric positive definite matrix. The Lyapunov function V for the overall system in Eqs. (10) and (11) is then taken to be the sum

$$V(x, z) = V_1(x) + V_2(z) = \frac{1}{2}x^T Q_x x + \frac{1}{2}z^T Q_z z. \tag{22}$$

[b] It is assumed that $\dot{V}_1 < 0$ in $\mathcal{D}_x \setminus \{0\}$ along the solution trajectories to Eq. (6) so that 0 is a $\mathcal{D}_x$-globally asymptotically stable equilibrium for this system, cf. [15, Thm. 4.2,4.4].

With this choice of Lyapunov function the time derivative along the solution trajectories to Eqs. (10) and (11) is

$$\dot{V}(x,z) = x^T Q_x \left(f(x) + G(x)(z+\mu(x))\right) + z^T Q_z \left(\tilde{h}(x,z) + Ku - \frac{\partial \mu(x)}{\partial x}\left(f_d(x) + G(x)z\right)\right) \tag{23}$$

$$\begin{aligned} &= x^T Q_x f_d(x) + x^T Q_x G(x) z \\ &\quad + z^T Q_z \tilde{h}(x,z) - z^T Q_z \frac{\partial \mu(x)}{\partial x} f_d(x) - z^T Q_z \frac{\partial \mu(x)}{\partial x} G(x) z + z^T Q_z K u, \end{aligned} \tag{24}$$

where we have used Eq. (5).

Control Law. The first term on the right in Eq. (24) is negative definite by assumption and the term containing u is linear in z. Since the remaining terms on the right in Eq. (24) also are either linear or quadratic in z, they can be partially or fully canceled by a control to render the right hand side of Eq. (24) negative definite. One such[c] (fully canceling) control law ν for u is

$$\nu(x,z) = K^{-1} Q_z^{-1} \left(-G^T(x) Q_x x - Q_z \tilde{h}(x,z) + Q_z \frac{\partial \mu(x)}{\partial x} f_d(x) + Q_z \frac{\partial \mu(x)}{\partial x} G(x) z - Q_2 z \right), \tag{25}$$

where Q_2 is a square symmetric positive definite matrix.

For later use we write down the linearization ν_ℓ of the control law ν in Eq. (25) around $(x,z) = (0,0)$, which is

$$\nu_\ell(x,z) = K^{-1} Q_z^{-1} \left(-G^T Q_x v - Q_z (Ex + Fz) + Q_z G^{-1} (A_d - A)(A_d x + Gz) - Q_2 z \right), \tag{26}$$

or, in matrix-vector form,

$$\nu_\ell(x,z) = -C_{\text{BBS}} \begin{bmatrix} x \\ z \end{bmatrix},$$

where $C_{\text{BBS}} \in \mathbb{R}^{3\times 6}$ is the static feedback gain matrix

$$C_{\text{BBS}} = -K^{-1} \begin{bmatrix} -Q_z^{-1} G^T Q_x - E + G^{-1}(A_d - A) A_d & -F + G^{-1}(A_d - A) G - Q_z^{-1} Q_2 \end{bmatrix}. \tag{27}$$

III.A.2. Stability

With the choice of control law ν as in Eq. (25) inserted in Eq. (24) we obtain

$$\dot{V}(x,z) = x^T Q_x f_d(x) - z^T Q_2 z < 0, \quad (x,z) \in \mathcal{D} \setminus \{(0,0)\}. \tag{28}$$

Hence, semiglobal stability follows from standard Lyapunov theory [15, Ch. 4]; the domain of attraction of $(0,0)$ includes the largest level set to the Lyapunov function V included in $\mathcal{D}$.

III.A.3. Closed loop system

The closed loop system obtained when applying the control law ν in Eq. (25) in lieu of u in Eqs. (10) and (11) is

$$\dot{x} = f_d(x) + G(x) z, \tag{29}$$

$$\dot{z} = -Q_z^{-1} G^T(x) Q_x x - Q_z^{-1} Q_2 z. \tag{30}$$

[c] One can also select Q_2 such that $-Q_2$ is Hurwitz and one can dominate, rather than cancel, some of the unwanted terms in the Lyapunov function time derivative in Eq. (24).

Linearized closed loop system. Linearizing the closed loop equations around $(x, z) = (0, 0)$ yields

$$\dot{x} = A_d x + Gz, \tag{31}$$

$$\dot{z} = -Q_z^{-1} G^T Q_x x - Q_z^{-1} Q_2 z. \tag{32}$$

For later reference we write down the corresponding system matrix $\tilde{A}_{\text{BBS}}$ which is given by

$$\tilde{A}_{\text{BBS}} = \begin{bmatrix} A_d & G \\ -Q_z^{-1} G^T Q_x & -Q_z^{-1} Q_2 \end{bmatrix}. \tag{33}$$

By construction, $\tilde{A}_{\text{BBS}}$ is Hurwitz but it is also intuitively clear that this must be the case in the limit when the off-diagonal elements are small and $-Q_2$ has all its eigenvalues sufficiently far out to the left on the real line. For the NDI controller below, the Hurwitz property of the corresponding system matrix is not unequivocally guaranteed, but requires some conditions (and a proof, such as the one in the appendix or in Ref. 16, which can be understood by a similar intuitive argument about the eigenvalues of a submatrix sufficiently far out in the left half of the complex plane).

III.B. Nonlinear dynamic inversion

The nonlinear dynamic inversion (by time scale separation) design does not explicitly use a Lyapunov function and the design moreover does not automatically generate a stability proof and stability region. Instead, it relies on a time scale separation assumption between the velocity and angular rate subsystems which can be shown to yield stability for the closed loop system.

III.B.1. Design procedure

Step 1. The first step in the NDI design procedure is identical to that of BBS except that the Lyapunov function V_1 is never used.

Step 2. In the second step, a linear form of the dynamics of the angular rate subsystem in Eq. (4) is postulated, and from this the control law η is derived. In detail, it is postulated that[d]

$$\dot{\omega} = A_\omega(\omega - \mu(x)), \tag{34}$$

where $A_\omega \in \mathbb{R}^{3\times 3}$ is Hurwitz.

Control law. From Eq. (4) we know that

$$\dot{\omega} = h(x, \omega) + Ku,$$

so this equation and Eq. (34) can be used to solve for the control u. The solution, denoted by η, is given by

$$\eta(x, \omega) = K^{-1} \left(A_\omega(\omega - \mu(x)) - h(x, \omega) \right).$$

The control law η can also be expressed as a function $\tilde{\eta}$ of the variables (x, z) as

$$\tilde{\eta}(x, z) = \eta(x, z + \mu(x)),$$

and we then have

$$\tilde{\eta}(x, z) = K^{-1} \left(A_\omega z - \tilde{h}(x, z) \right). \tag{35}$$

Here, the desired dynamics f_d do not enter explicitly in the control law (as in the BBS case), only implicitly in terms of the definition of the zero error manifold $z = 0$.

For later use we write down the linearization $\tilde{\eta}_\ell$ of the control law $\tilde{\eta}$ in Eq. (35) around $(x, z) = (0, 0)$, which is

$$\tilde{\eta}_\ell(x, z) = K^{-1} \left(A_\omega z - (Ex + Fz) \right),$$

[d]Nonlinear dynamics could also be postulated, but this is rarely done. It is moreover clear here that the postulated dynamics makes sense intuitively if $\mu(x)$ can be considered as a slowly time varying function compared to z, a reference signal.

or, on matrix-vector form,

$$\tilde{\eta}_\ell(x,z) = -C_{\text{NDI}} \begin{bmatrix} x \\ z \end{bmatrix}$$

where $C_{\text{NDI}} \in \mathbb{R}^{3\times 6}$ is the matrix

$$C_{\text{NDI}} = -K^{-1}\begin{bmatrix} -E & A_\omega - F \end{bmatrix}. \tag{36}$$

III.B.2. Closed loop system, stability

The equations for the closed loop system obtained when the control law $\tilde{\eta}$ in Eq. (35) is substituted for u in Eqs. (10) and (11) are immediately obtained as

$$\dot{x} = f_d(x) + G(x)z, \tag{37}$$

$$\dot{z} = A_\omega z - \frac{\partial \mu}{\partial x}(f_d(x) + G(x)z). \tag{38}$$

With the choice $A_\omega = -Q_z^{-1}Q_2$ this system becomes similar to the closed loop BBS system in Eqs. (31) and (32) and similar Lyapunov analysis can be applied. It is then possible to show that the unwanted terms that appear in a quadratic Lyapunov function can be dominated by making the eigenvalues of A_ω lie sufficiently far out in the left hand plane.[e]

Linearized closed loop system. The linearization of the closed loop system in Eqs. (37) and (38) around $(x,z) = (0,0)$ is

$$\dot{x} = A_d x + Gz,$$
$$\dot{z} = A_\omega z - G^{-1}(A_d - A)(A_d x + Gz).$$

The system matrix $\tilde{A}_{\text{NDI}}$ for this system is

$$\tilde{A}_{\text{NDI}} = \begin{bmatrix} A_d & G \\ -G^{-1}(A_d - A)A_d & A_\omega - G^{-1}(A_d - A)G \end{bmatrix} \tag{39}$$

and it is not difficult to show (see the appendix) that, under some not very restrictive conditions on A_d, A_ω, it can be made strict Hurwitz by placing the eigenvalues of the symmetric part of A_ω sufficiently far out to the left in the complex plane.

IV. Time Scale Separation

The NDI method relies on time scale separation (in the closed loop) between the slow x-system and the fast z-system for its stability. The BBS method, on the other hand, does not need this condition for stability but its performance can be improved with increased time scale separation. It is therefore of interest to examine more closely the effects of varying degrees of time scale separation for both methods. In order to do this consistently we need a way to characterize time scale separation more precisely and in a way that applies to both methods.

In the application on which we focus the dynamics are only weakly nonlinear around the origin (the equilibrium) and therefore linear analysis will provide relevant information. Moreover, using linear theory offers several ways of easily and efficiently characterizing time scale separation. If we restrict ourselves to the case where BBS and NDI are related as $A_\omega = -Q_z^{-1}Q_2$ (where A_ω is Hurwitz) it is natural to define the time scale separation factor TSS as

$$\text{TSS} = \frac{\min|\lambda(A_\omega)|}{\max|\lambda(A_d)|}, \tag{40}$$

assuming also A_d is Hurwitz.

To intuitively illustrate the mechanisms at work we shall first look at two simple examples for the pitch channel[f] and then give a couple of more general definitions of time scale separation. These two definitions are then further investigated numerically for a real vehicle with BBS and NDI controller in Sec. VI.

[e] This can be said to be the method employed by Schumacher et al.[16] to prove stability for NDI.

[f] We continue to use notation of the type introduced in Sec. II for the full six degree of freedom problem for the pitch channel examples considered here; the adaptations made should be obvious.

IV.A. Stability and time scale separation for the pitch channel: I

Consider the pitch channel dynamics around an equilibrium (trim) point, without loss of generality set at $\alpha = 0$. By retaining only the most important terms from Eqs. (1) and (2) we obtain the following simple model of these dynamics,

$$\dot{\alpha} = f_z(\alpha) + q, \tag{41}$$
$$\dot{q} = m_\alpha(\alpha) + m_q(q) + u, \tag{42}$$

where f_z is normalized force along the z-axis in the body frame, $m_\alpha(\alpha)$ is the normalized pitch moment due to angle of attack α, $m_q(q)$ is the normalized pitch damping due to pitch rate q, and u is the normalized pitch control moment due to control surface deflections. It is assumed that $f_z(0) = m_\alpha(0) = m_q(0) = 0$. Suppose that there is given a desired normalized lift $f_z^{(d)}$ that is to be realized locally around $\alpha = 0$ by dynamics synthesis using backstepping or NDI. The virtual control law $q^{(d)}$ is then given by

$$q^{(d)}(\alpha) = f_z^{(d)}(\alpha) - f_z(\alpha),$$

and the system in Eqs. (41) and (42) rewritten on error form using $\tilde{q} = q - q^{(d)}$ becomes

$$\dot{\alpha} = f_z^{(d)}(\alpha) + \tilde{q}, \tag{43}$$
$$\dot{\tilde{q}} = m_\alpha(\alpha) + \tilde{m}_q(\alpha, \tilde{q}) + u - \frac{dq^{(d)}(\alpha)}{d\alpha}\left(f_z^{(d)}(\alpha) + \tilde{q}\right), \tag{44}$$

where

$$\tilde{m}_q(\alpha, \tilde{q}) = m_q(\tilde{q} + q^{(d)}(\alpha)).$$

Backstepping and NDI control laws ν_{BS} and ν_{NDI}, respectively, are then easily constructed as special cases of those outlined in Secs. III.A.1 and III.B.1 as

$$\nu_{\mathrm{BS}}(\alpha, \tilde{q}) = -m_\alpha(\alpha) - \tilde{m}_q(\alpha, \tilde{q}) + \frac{dq^{(d)}(\alpha)}{d\alpha} f_z^{(d)}(\alpha) + \frac{dq^{(d)}(\alpha)}{d\alpha}\tilde{q} - \frac{Q_\alpha}{Q_{\tilde{q}}}\alpha - Q_2\tilde{q}$$

and

$$\nu_{\mathrm{NDI}}(\tilde{q}) = -m_\alpha(\alpha) - \tilde{m}_q(\alpha, \tilde{q}) + a_q\tilde{q},$$

where $Q_{\tilde{q}}$ and Q_α are positive weighting constants and $-Q_2$ and a_q are negative scalar coefficients for the desired linear dynamics of the error $\tilde{q}$. We use the same desired error dynamics for both methods, i.e. we set $Q_2 = -a_q$, in order to isolate the effects of time scale separation. Furthermore, we set $Q_\alpha = \varepsilon Q_{\tilde{q}}$, where $\varepsilon > 0$ is small, making the synthesized inter-subsystem coupling term $\frac{Q_\alpha}{Q_{\tilde{q}}}\alpha$ negligible while still maintaining Lyapunov stability[g] for the backstepping control law. Using these control laws and constants, the closed loop system for backstepping is

$$\dot{\alpha} = f_z^{(d)}(\alpha) + \tilde{q},$$
$$\dot{\tilde{q}} = a_q\tilde{q} - \varepsilon\alpha,$$

and for NDI it is

$$\dot{\alpha} = f_z^{(d)}(\alpha) + \tilde{q},$$
$$\dot{\tilde{q}} = a_q\tilde{q} - \frac{dq^{(d)}(\alpha)}{d\alpha}\left(f_z^{(d)}(\alpha) + \tilde{q}\right).$$

As an example, we consider a case where the linearized dynamics are identical with those for the pitch channel in the example in Sec. VI.A below but where f_z has a prescribed quadratic nonlinear form. More precisely, we set

$$f_z(\alpha) = \alpha(1.1\alpha - 0.954) \quad \text{for} \quad \alpha \geq 0,$$
$$f_z(\alpha) = -f_z(-\alpha) \quad \text{for} \quad \alpha < 0,$$

[g] As was mentioned in Sec. III.B.2, NDI can be made stable in the sense of Lyapunov given an a_q large enough to be able to dominate the over second term in the $\tilde{q}$ dynamics. This is in fact the requirement for time scale separation.

so that $A = -0.954$ and prescribe linear dynamics that are roughly twice as fast as the inherent dynamics around the origin, i.e.

$$f_z^{(d)}(\alpha) = -2\alpha \tag{45}$$

so that $A_d = -2$. The functions f_z and $f_z^{(d)}$ are shown in Fig. 1. For illustrative purposes, the nonlinearity in f_z and the significant difference between $f_z^{(d)}$ and f_z have been exaggerated. In a purely realistic setting, control authority would limit one's choice of $f_z^{(d)}$. With these parameters the time scale separation factor

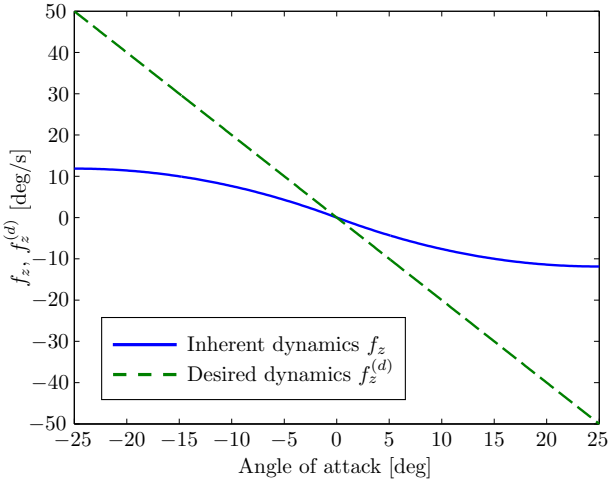

Figure 1. Open loop dynamics and desired closed loop dynamics.

TSS in Eq. (40) becomes

$$\text{TSS} = -\frac{a_q}{2}.$$

In Fig. 2 the resulting vector field of the closed loop system resulting from backstepping and NDI is shown for two different values of the time scale separation factor TSS. When $Q_2 = -a_q = 10$, so that TSS=5, the large difference in prescribed time scales is manifested differently in the backstepping and NDI closed loop vector fields. The backstepping controller synthesizes the different time scales in the closed loop system,

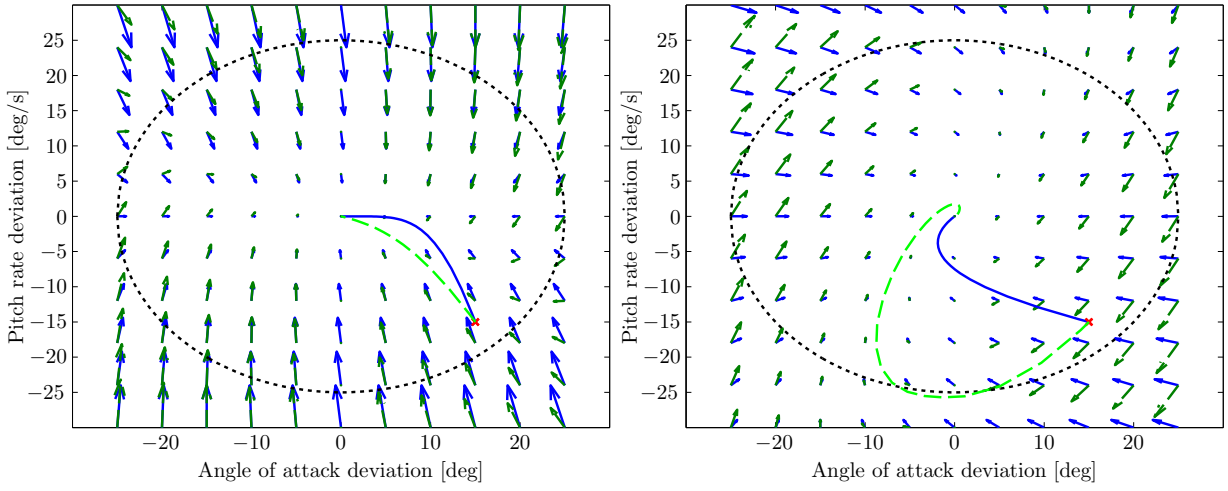

Figure 2. Backstepping (——>) and NDI (– –>) closed loop vector fields with $a_q = -10$ giving a time scale separation factor TSS of 5 (left) and with $a_q = -1$ yielding a TSS value of 0.5 (right). The Lyapunov function level set is a circle (------), corresponding to using the 2-norm as the Lyapunov function. Example trajectories are shown for backstepping (——) and NDI (– – –) controllers, with initial points marked in red.

giving rise to trajectories similar to the one shown in the figure (fast pitch rate dynamics, slower angle of attack dynamics). The NDI controller, on the other hand, relies on the different time scales to synthesize stable dynamics, which in turn are not guaranteed to have any time scale separation. Indeed, from the example trajectory shown in the figure, though stable, the NDI controller does not appear to have created

any significant time scale separation. Decreasing the time scale separation emphasizes these effects. For example, when decreasing $Q_2 = -a_q$ to 1 so that TSS=0.5 (i.e. no significant time scale separation), the backstepping controller still performs adequately (as expected), whereas the vector field created by the NDI controller appears to have rotated significantly away from the origin, leading to the large excursion in the example trajectory.

IV.B. Stability and time scale separation for the pitch channel: II

It is instructive to look at the eigenvalues of the linearized closed loop systems in two dimensions, such as the pitch channel case considered above. Suppose the linearized open loop dynamics are unstable so that A in Eq. (12) is given by a positive number $A > 0$ and the desired dynamics A_d by a negative number $A_d = -|A_d| < 0$. Set $G = Q_z = 1$ (without loss of generality) and rename A_ω to $-Q_2$. The variables Q_x and Q_2 are both strictly positive.

The eigenvalues for $\tilde{A}_{\mathrm{BBS}}$ in Eq. (33) are then given by

$$\lambda_{\mathrm{BBS}} = -\frac{1}{2}(Q_2 + |A_d|) \pm \frac{1}{2}\sqrt{(Q_2 - |A_d|)^2 - 4Q_x}. \tag{46}$$

Clearly, the real part of λ_{BBS} is always negative (as expected, since BBS yields a stable closed loop system by construction), indeed $-\max\{Q_2, |A_d|\} \leq \mathrm{Re}(\lambda_{\mathrm{BBS}}) \leq -\min\{Q_2, |A_d|\}$. The eigenvalues λ_{BBS} become complex if Q_x is too large as compared to the difference between the diagonal terms Q_2 and $|A_d|$.

For $\tilde{A}_{\mathrm{NDI}}$ in Eq. (39), the eigenvalues are given by

$$\lambda_{\mathrm{NDI}} = -\frac{1}{2}(Q_2 - A) \pm \frac{1}{2}\sqrt{(Q_2 - A)^2 - 4\,|A_d|\,Q_2}. \tag{47}$$

Here, the real part of λ_{NDI} is strictly negative if and only if $Q_2 > A$. This may be stated as a condition for time scale separation. Note that this condition involves the *original* open loop dynamics A, and not the desired A_d. The NDI modes are oscillatory if and only if

$$(Q_2 - A)^2 - 4\,|A_d|\,Q_2 < 0 \tag{48}$$

i.e. if and only if

$$(Q_2 - A)^2 - 4\,|A_d|\,(Q_2 - A) - 4\,|A_d|\,A < 0.$$

The roots to the polynomial in $Q_2 - A$ on the left are

$$(Q_2 - A)_{1,2} = 2\,|A_d|\,(1 \pm \sqrt{1 + A/\,|A_d|}).$$

It is easy to verify that Eq. (48) is fulfilled for $Q_2 - A$ in the open interval defined by these roots (the extent of which is proportional to the size of the desired dynamics coefficient $|A_d|$), but not outside it. Thus, in particular, the modes are oscillatory when the desired dynamics are too fast compared to the time scale separation $Q_2 - A$, or conversely when the time scale separation is not large enough to match the desired dynamics.

The presence of A in Eq. (47) shows that NDI does not manage to fully compensate for the original dynamics. Also, avoiding oscillatory solutions is a simple matter for backstepping but a more involved one for NDI.

V. Sensitivity

For a weakly nonlinear system, information about many important properties of the closed loop can be obtained from a classical sensitivity analysis of the linearized closed loop system.

V.A. Transfer function of linearized closed loop system

In order to perform a sensitivity analysis we introduce a new reference signal $\tilde{r}$, with values in $\mathbb{R}^3$, and consider the closed loop transfer function MHN from $\tilde{r}$ to $y = M\xi$, via $r = N\tilde{r}$, with $\xi = (x, z)$ and M, N as in Eqs. (19), (20). The factor H of the transfer function MHN is given by

$$H(s) = (sI_6 - (A_e - B_eC))^{-1}\,B_eC = (sI_6 - \tilde{A})^{-1}B_eC \tag{49}$$

where $(\tilde{A}, C)$ is either $(\tilde{A}_{\rm BBS}, C_{\rm BBS})$ in Eq. (33), (27) or $(\tilde{A}_{\rm NDI}, C_{\rm NDI})$ in Eq. (39), (36). The factor H can be written on unit negative feedback form in terms of the open loop plant transfer function P in Eq. (18) as

$$H(s) = \left(I_6 + (sI_6 - A_e)^{-1}B_eC\right)^{-1}(sI_6 - A_e)^{-1}B_eC = (I_6 + P(s)C)^{-1}P(s)C. \tag{50}$$

A block diagram of the system MHN on unit negative feedback form is shown in Fig. 3 where also an output disturbance n with values in $\mathbb{R}^3$ is added as well as a load disturbance ℓ with values in $\mathbb{R}^3$.

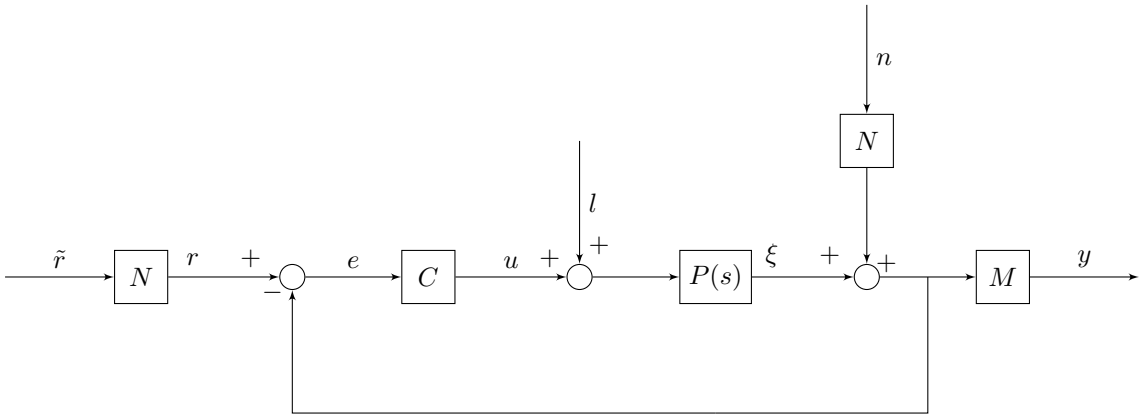

Figure 3. Block diagram of the system in Eq. (18) with the controller in Eq. (27) in standard feedback form. The reference signal r is 0 in the set point control problem we consider and the state vector ξ is given by $\xi = (x, z)$.

V.B. Output sensitivity

The transfer function H in Eqs. (49) and (50) is identical with the *output sensitivity function* O and can be factored in terms of the *sensitivity function* S and (open) *loop gain* Γ given by

$$S(s) = (I_6 + P(s)C)^{-1} \quad \text{and} \quad \Gamma(s) = P(s)C. \tag{51}$$

The *load sensitivity function* L finally is given by

$$L(s) = S(s)P(s). \tag{52}$$

The sensitivity function S in Eq. (51) gives a measure of the disturbance attenuation due to feedback. It relates the tracking error to the reference signal, and gives also an indication of the relative error in the closed loop transfer function due to modeling uncertainties. With the knowledge of P, C, and S, a number of robustness properties of the closed loop system can be obtained.[17] Since the sensitivity function S also appears as a factor in L we shall here concentrate on S.

In Sec. VI below, the sensitivity functions S and L are evaluated for an RLV with BBS and NDI controllers.

V.B.1. Optimizing the low frequency sensitivity

From Eq. (18) it follows that the low frequency limit $S(0)$ of the sensitivity function in Eq. 51 has the simple analytical expression

$$S(0) = (I_6 - A_e^{-1}B_eC)^{-1} = (A_e - B_eC)^{-1}A_e = \tilde{A}^{-1}A_e.$$

The matrix $\tilde{A}$ on the right contains the parameters from the control law $C_{\rm BBS}$ or $C_{\rm NDI}$ and by using this representation for $S(0)$ various strategies for optimizing different aspects of $S(0)$ by selection of the control law parameters can be developed. In the general case such a program is difficult to carry out analytically (although it can be done numerically, cf. Sec. VI below) but in the 2×2 case, such as in the pitch channel setting discussed above, this is fairly strightforward to do as we show below.

The linearized BBS control law $C_{\rm BBS}$ in Eq. (27) is parametrized in terms of the three matrices Q_x, Q_z, and Q_2, all three of which can be used to optimize sensitivity. The linearized NDI control law $C_{\rm NDI}$ in Eq. (36) is parametrized in terms of A_ω, which can be used for sensitivity optimization. However, in order to

make the sensitivity optimization problem meaningful it is reasonable to fix some parameters, for instance the desired synthesized dynamics for the z-system. Then there are no parameters left to vary for the NDI control law and for the BBS control law it is required that the product $-Q_z^{-1}Q_2$ is fixed at some value A_ω, where A_ω is Hurwitz (like in Sec. IV). Under this assumption we shall now show how optimization can be carried out in the 2×2 case for the BBS control law.

THE 2×2 CASE. When $\tilde{A}_{\text{BBS}}, A_e \in \mathbb{R}^{2\times 2}$ we have

$$\tilde{A}_{\text{BBS}}^{-1} A_e = \frac{1}{G^2 Q_x/Q_z - A_d Q_2/Q_z} \begin{bmatrix} -A_d Q_2/Q_z - EG + (A_d - A)A_d & -GQ_2/Q_z - FG + (A_d - A)G \\ A_d G Q_x/Q_z + EA_d - (A_d - A)A_d^2/G & G^2 Q_x/Q_z + FA_d - (A_d - A)A_d \end{bmatrix}, \quad (53)$$

provided

$$G^2 Q_x/Q_2 - A_d \neq 0. \quad (54)$$

Assuming that Eq. (54) holds, the lower left corner of the matrix on the right in Eq. (53) can be made zero by proper selection of Q_x if and only if

$$\frac{Q_x}{Q_z} = -\frac{E}{G} + \frac{(A_d - A)A_d}{G^2} \in (0, \infty). \quad (55)$$

The right part of the condition is equivalent to

$$EG - (A_d - A)A_d < 0. \quad (56)$$

Similarly, the lower right corner of the matrix on the right in Eq. (53) can be made zero by proper selection of Q_x if and only if

$$\frac{Q_x}{Q_z} = \frac{-FA_d + (A_d - A)A_d}{G^2} \in (0, \infty). \quad (57)$$

Since $A_d < 0$, the right part of this condition is equivalent to

$$-F + A_d - A < 0. \quad (58)$$

V.C. Optimizing the low frequency sensitivity for the pitch channel

The linearization around $(\alpha, \tilde{q}) = (0, 0)$ of the open loop error system in Eqs. (43),(44) for the pitch plane dynamics is (cf. Eqs. (13),(14))

$$\begin{bmatrix} \dot{\alpha} \\ \dot{\tilde{q}} \end{bmatrix} = \begin{bmatrix} A_d & 1 \\ E - (A_d - A)A_d & F - A_d + A \end{bmatrix} \begin{bmatrix} \alpha \\ \tilde{q} \end{bmatrix} + \begin{bmatrix} 0 \\ 1 \end{bmatrix} u,$$

where $A, E, F \in \mathbb{R}$ and $A_d < 0$ are given by (cf. Eqs. (15),(16))

$$\begin{aligned} A &= \left.\frac{df_z(\alpha)}{d\alpha}\right|_{\alpha=0}, \\ E &= \left.\frac{dm_\alpha(\alpha)}{d\alpha}\right|_{\alpha=0} + \left.\frac{dm_q(q)}{dq}\right|_{q=0} \left.\frac{dq^{(d)}(\alpha)}{d\alpha}\right|_{\alpha=0} = \left.\frac{dm_\alpha(\alpha)}{d\alpha}\right|_{\alpha=0} + F(A_d - A), \\ F &= \left.\frac{dm_q(q)}{dq}\right|_{q=0}, \\ A_d &= \left.\frac{df_z^{(d)}(\alpha)}{d\alpha}\right|_{\alpha=0}. \end{aligned}$$

The condition in Eq. (56) for nulling the lower left corner of $S(0)$ thus becomes

$$\left.\frac{dm_\alpha(\alpha)}{d\alpha}\right|_{\alpha=0} + (F - A_d)(A_d - A) < 0. \quad (59)$$

Since the first term, the pitch stiffness derivative, is negative for a naturally (statically) stable aircraft it is clear that a minimizer as in Eq. (55) will always exist provided $|(F - A_d)(A_d - A)|$ is sufficiently small. A straightforward way to guarantee this is to choose $A_d = A$. Another obvious way to guarantee that Eq. (59) is fulfilled is to make $|A_d|$ sufficiently large.

The condition in Eq. (57) for nulling the lower right corner of $S(0)$ can be written

$$\left.\frac{dm_q(q)}{dq}\right|_{q=0} - A_d + A > 0, \tag{60}$$

where we note that the first term on the left, the pitch damping derivative, is always negative. Thus, it is clear that the condition for nulling the lower right corner of $S(0)$ can not be fulfilled with the choice $A_d = A$ but can always be fulfilled by making A_d sufficiently large. Summing up, minimization of either of the two lower corners of $S(0)$ is always possible by making A_d sufficiently large (although this may not always be a desirable strategy).

For the pitch channel in the example in Sec. VI.A we have

$$A = -0.9540, \quad E = -5.5481, \quad F = -0.5901, \quad A_d = -1, \tag{61}$$

and therefore it follows that for that example,

$$\left.\frac{dm_\alpha(\alpha)}{d\alpha}\right|_{\alpha=0} = -5.5752.$$

A simple check reveals that Eq. (59) is fulfilled in this example, so that a minimizing ratio Q_x/Q_z as in Eq. (55) exists (and Eq. (54) is fulfilled), but Eq. (60) is not fulfilled.

VI. Simulation Results

VI.A. The ALPHA reusable launch vehicle

The ALPHA, or Airplane Launched Phoenix Aircraft, is a suborbital RLV whose development is funded by the European Space Agency as part of the Future high-Altitude high-Speed Transport 20XX (FAST20XX) program. Its design is intended as a means for evaluating the possibilities of future high-altitude travel, in particular for the purpose of space tourism.

The results that follow are based on aerodata on the ALPHA collected in wind tunnel experiments as well as from computational fluid dynamic calculations. The simulations are set at an altitude of 3 km at Mach number 0.32 with a flight path angle of $-23°$. Numerical linearization using the ALPHA's aerodata results in the matrices (see Sec. II.D for definitions)

$$A = \begin{bmatrix} -0.9540 & -0.0083 & 0 \\ 0 & -0.5627 & 0.0832 \\ 0 & 0 & 0 \end{bmatrix}, \qquad G = \begin{bmatrix} 0 & 1.0000 & 0 \\ 0.1052 & 0 & -0.9944 \\ 1.0000 & 0 & -0.3144 \end{bmatrix},$$

$$E = \begin{bmatrix} 0.0046 & -35.9477 & 0 \\ -5.5481 & -2.1663 & 0 \\ 0.0001 & 5.0076 & 0 \end{bmatrix}, \qquad F = \begin{bmatrix} -4.2029 & 0.0005 & 4.8343 \\ 0.0006 & -0.5901 & -0.0007 \\ 0.3815 & 0.0000 & -1.0862 \end{bmatrix},$$

and the gain matrix K is

$$K = J^{-1} = 10^{-3} \begin{bmatrix} 0.8342 & -0.0001 & 0.0112 \\ -0.0001 & 0.1461 & 0.0000 \\ 0.0112 & 0.0000 & 0.1482 \end{bmatrix}.$$

The desired dynamics matrix A_d is set to $-I_3$, which, when considering simplifications of the short period, Dutch roll, and roll subsidence modes, fulfills the ubiquitous US Department of Defense handling quality requirements.[18]

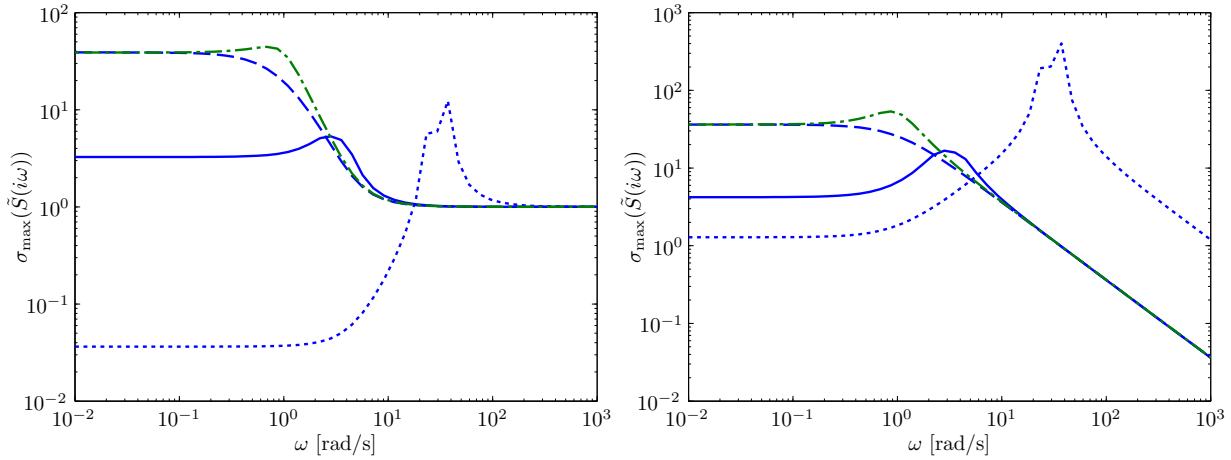

(a) $M_1(I_6 + P(s)C)^{-1}N_1$ (n_x to x)

(b) $M_2(I_6 + P(s)C)^{-1}N_1$ (n_x to z)

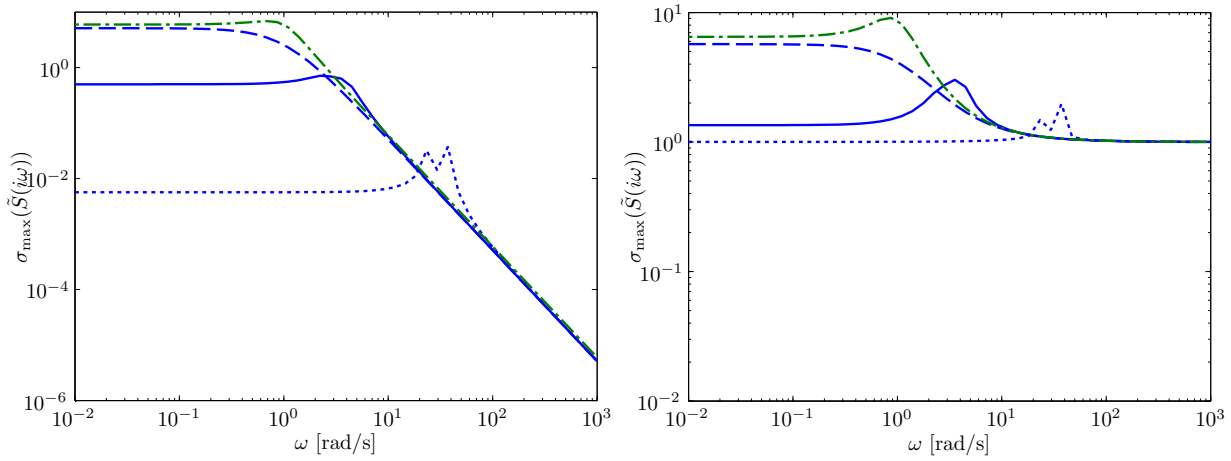

(c) $M_1(I_6 + P(s)C)^{-1}N_2$ (n_z to x)

(d) $M_2(I_6 + P(s)C)^{-1}N_2$ (n_z to z)

Figure 4. Sensitivity S for the ALPHA at altitude 3 km and Mach number 0.32 with BBS controllers parametrized by $Q_x = 0.001I_3$ (– – –), $Q_x = 10I_3$ (——), and $Q_x = 1000I_3$ (·····), and an NDI controller (– · –). The time scale separation factor TSS between the slow and fast loops is 1.

VI.B. Sensitivity for the ALPHA with BBS and NDI controllers

Figures 4 and 5 present the sensitivity S in Eq. (51) for the ALPHA model, linearized at the point of the envelope described above, for both BBS and NDI controllers. The desired dynamics for the x-system is $A_d = -I_3$ and the z-system gains are equal for both controllers, $A_\omega = -Q_2$ (Q_z is set to I), cf. Eqs. (33) and (39).

In each panel, the largest singular value $\sigma_{\max}$ is plotted for a certain 3×3 sub-block $\tilde{S}(i\omega) = M_j S(i\omega) N_k$ of the sensitivity $S(i\omega)$. For BBS, graphs for three different values of the x-gains Q_x are given. The two figures show the results for different values of the time scale separation factor TSS (obtained for $Q_2 = I$ and $Q_2 = 10I$ respectively), both of which result in NDI matrices $\tilde{A}_{\text{NDI}}$ that are strictly Hurwitz.

The general shape of the curves at high frequencies is as expected, i.e. the 12 dB/octave roll-off for the cross channels and the constant plateau for the diagonal blocks. The effect of increasing TSS is not very large, indicating a small latitude for NDI to change the sensitivity (since this is the only parameter).

For BBS, on the other hand, Q_x is clearly available to shape S. A high value of Q_x can give a significant reduction of the low frequency sensitivity in the left panels, at the expense of an increase at high frequencies in the upper right panels.

At high time scale separation, the NDI controller synthesizes dynamics fast enough to keep the fast error system close to 0, making the slow subsystems of the BBS and NDI controllers very similar. As a result, disturbances are attenuated quicker and their effects on the slow subsystem minimized. This is apparent

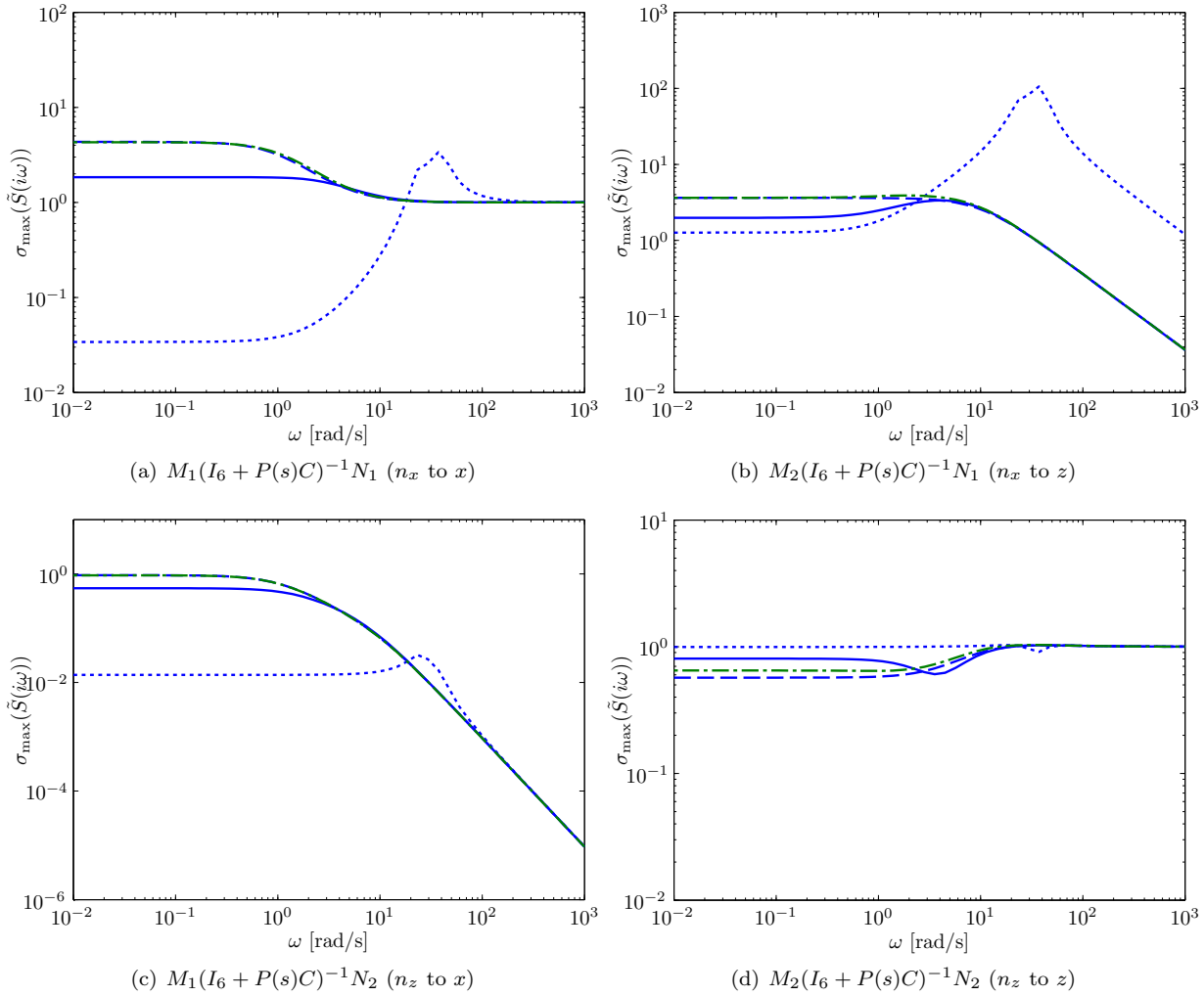

(a) $M_1(I_6 + P(s)C)^{-1}N_1$ (n_x to x)

(b) $M_2(I_6 + P(s)C)^{-1}N_1$ (n_x to z)

(c) $M_1(I_6 + P(s)C)^{-1}N_2$ (n_z to x)

(d) $M_2(I_6 + P(s)C)^{-1}N_2$ (n_z to z)

Figure 5. Sensitivity S for the ALPHA at altitude 3 km and Mach number 0.32 with BBS controllers parametrized by $Q_x = 0.001I_3$ (– – –), $Q_x = 10I_3$ (——), and $Q_x = 1000I_3$ (·····), and an NDI controller (– · –). The time scale separation factor TSS between the slow and fast loops is 10.

in Figs. 5(a) and 5(c) where the significant time scale separation enables the NDI controller to produce sensititives nearly identical to those of the BBS controller parameterized by the small inter-subsystem factor $Q_x = 0.001I_3$.

While the difference in sensitivities of the slow subsystem is dependent predominantly on time scale separation, the difference in sensitivities of the fast subsystems is dependent (to a greater extent) on two more factors. Comparing the BBS sensitivity function $S_{\text{BBS}}(s) = (I_6 + P(s)C_{\text{BBS}})^{-1}$ with the NDI sensitivity function $S_{\text{NDI}}(s) = (I_6 + P(s)C_{\text{NDI}})^{-1}$, one can observe that they differ only in feedback matrices, which in turn differ only in terms of the BBS parameter Q_x and functions of the difference in prescribed and inherent dynamics $A_d - A$. This is apparent in Fig. 5(d) in the sensitivities of the NDI controller and the BBS controller parametrized by $Q_x = 0.001I_3$. In contrast to Figs. 5(a) and 5(c), there is a noticeable difference between the two, in this case primarily being due to the difference between desired and inherent dynamics.

The very different shape of the high-Q_x curve, with a discernible "resonance peak," may indicate the presence of oscillatory modes. This is consistent with the result for the two dimensional example in Sec. IV.B where λ_{BBS} in Eq. (46) becomes complex for large values of Q_x. By increasing Q_2 in Fig. 5, this "resonance" behavior is counteracted.

Resonance peaks are also exhibited by the NDI controllers. These appear when oscillatory modes occur due to insufficient time scale separation, which is consistent with the results in Sec. IV.B. Figure 4, where these is little time scale separation, shows these peaks (cf. Fig. 5 of high time scale separation where the resonance peaks are not present).

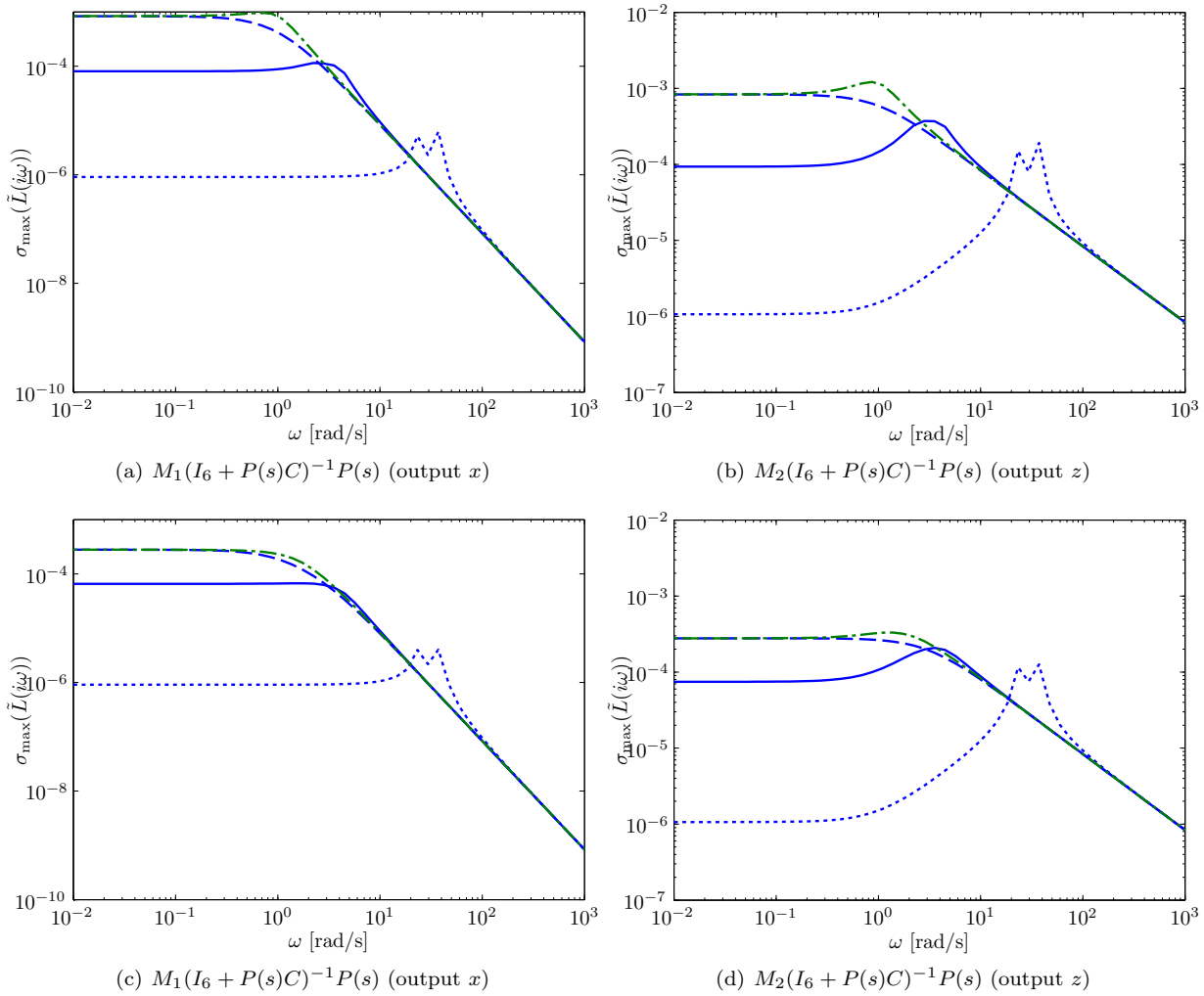

(a) $M_1(I_6 + P(s)C)^{-1}P(s)$ (output x)

(b) $M_2(I_6 + P(s)C)^{-1}P(s)$ (output z)

(c) $M_1(I_6 + P(s)C)^{-1}P(s)$ (output x)

(d) $M_2(I_6 + P(s)C)^{-1}P(s)$ (output z)

Figure 6. Load sensitivity L for the ALPHA at altitude 3 km and Mach number 0.32 with BBS controllers parametrized by $Q_x = 0.001I_3$ (– – –), $Q_x = 10I_3$ (——), and $Q_x = 1000I_3$ (·····), and an NDI controller (– · –). The time scale separation factor TSS between the slow and fast loops is 1 (top two panels) and 3 (bottom two panels) respectively.

In Fig. 6, finally, the behavior of the load sensitivity L in Eq. (52) is displayed for two different time scale separation factors. In each panel, the largest singular value $\sigma_{\max}$ is plotted for a certain 3×3 sub-block $\tilde{L}(i\omega) = M_j L(i\omega)$ of the load sensitivity $L(i\omega)$. The behavior is similar to that of S with the important difference that the trade-off between a lower low frequency sensitivity and high high frequency sensitivity that exist between the two cross channels is not present. Instead, there is a consistent lowering of the load sensitivity at lower frequencies when Q_x is increased at no significant expense at high frequencies, apart from an increase in the resonance peak height.

VII. Conclusions

We have compared certain stability and robustness properties for the two nonlinear design methods block backstepping and nonlinear dynamic inversion by time scale separation using linearization techniques of the closed loop system as a primary means of investigation. This is motivated by the fact that both the closed loop slow (velocity) subsystem and the fast (angular rate) subsystem is often approximately linear. Moreover, it enables the use of well known and intuitive analysis tools from linear analysis.

In particular, we have investigated stability and classical sensitivity properties (output and load sensitivity) and shown that there is a trade-off for both methods. The BBS method has more terms in the control law and we have shown that these give a higher degree of design freedom to balance this trade-off than for

the NDI method. In the sensitivity analysis, it is observed that at low gains of one of the BBS-specific terms, the BBS sensitivities do not differ substantially from their NDI counterparts. However, the intrinsic extra degree of freedom in the BBS controller enables the slow subsystem to be made less sensitive to disturbances at low frequencies at the (minor) expense of oscillatory modes. Since the primary objective is most often to have good tracking on the slow subsystem, this ability is seen as a valuable merit for BBS.

Furthermore, it is demonstrated that the extent of time scale separation plays a central role in the difference in behavior of the two methods. When designing an NDI controller, having sufficient time scale separation is vital to the stability of the closed loop system, while at the same time being the only design parameter controlling system performance (assuming the prescribed slow dynamics cannot be changed). In other words, system stability is guaranteed at the cost of reduced design freedom. Ultimately the large time scale separation is needed to dominate over terms not taken into account in the synthesis. This can lead to inherently slow systems being unnaturally fast, potentially causing adverse effects in the closed loop system, such as undesirable handling qualities. The BBS controller, on the other hand, guarantees stability and gives adequate performance regardless of the difference in time scales and without imposing extra restrictions on the remaining degrees of freedom, and in fact synthesizes the difference in the closed loop system. The effects this synthesis and other design choices have on control effort is not studied here, but need to be investigated to provide a more complete picture of the advantages and disadvantages of BBS in comparison to NDI.

Appendix

Here we show that, under conditions specified below, the matrix $\tilde{A}_{\text{NDI}}$ in Eq. (39) can be made Hurwitz by proper choice of A_d and A_ω in Eqs. (12) and (34), respectively.

Let $A_d \in \mathbb{R}^{3\times 3}$ be as in Eq. (12) (recall that A_d is Hurwitz by assumption). Define the symmetric part $A_d^{(s)}$ of A_d by

$$A_d^{(s)} = \frac{1}{2}(A_d + A_d^T).$$

Let $A_\omega \in \mathbb{R}^{3\times 3}$ be as in Eq. (34) and assume that A_ω is of the form

$$A_\omega = \gamma \tilde{A}_\omega \tag{62}$$

where $\gamma > 0$ and $\tilde{A}_\omega \in \mathbb{R}^{3\times 3}$ (which is Hurwitz like A_ω by assumption). Define the symmetric parts $\tilde{A}_\omega^{(s)}, A_\omega^{(s)}$ of $\tilde{A}_\omega, A_\omega$, respectively, as

$$\tilde{A}_\omega^{(s)} = \frac{1}{2}(\tilde{A}_\omega + \tilde{A}_\omega^T), \quad A_\omega^{(s)} = \frac{1}{2}(A_\omega + A_\omega^T) = \gamma \tilde{A}_\omega^{(s)},$$

and likewise define the symmetric part $\tilde{A}_{\text{NDI}}^{(s)} \in \mathbb{R}^{3\times 3}$ of $\tilde{A}_{\text{NDI}}$ in in Eq. (39) by

$$\tilde{A}_{\text{NDI}}^{(s)} = \frac{1}{2}(\tilde{A}_{\text{NDI}} + \tilde{A}_{\text{NDI}}^T).$$

For the Proposition below we shall need the following simple fact about definiteness for partitioned matrices. If Q, R, S are matrices of compatible dimensions, where Q, R are symmetric, then the matrix M given by

$$M = \begin{bmatrix} Q & S \\ S^T & R \end{bmatrix} \tag{63}$$

is negative definite if and only if both R and $Q - SR^{-1}S^T$ are negative definite. This follows immediately by considering the quadratic form

$$(x, u) \mapsto x^T Q x + 2x^T S u + u^T R u = (u + R^{-1}S^T x)^T R (u + R^{-1}S^T x) + x^T (Q - SR^{-1}S^T)x.$$

For the spectrum $\lambda(T)$ of an arbitrary matrix $T \in \mathbb{R}^{n\times n}$ we also recall the following estimate

$$\lambda_{\min}\left(\frac{1}{2}(T + T^T)\right) \le \text{Re}(\lambda(T)) \le \lambda_{\max}\left(\frac{1}{2}(T + T^T)\right). \tag{64}$$

This estimate is well-known, see e.g. [19, Sec. 1.2].

Proposition. Assume that both $A_d^{(s)}$ and $\tilde{A}_\omega^{(s)}$ are negative definite. Then, for sufficiently large γ in Eq. (62), the matrix $\tilde{A}_{\text{NDI}}$ in Eq. (39) is Hurwitz.

Proof. We have

$$\tilde{A}_{\text{NDI}}^{(s)} = \begin{bmatrix} A_d^{(s)} & \frac{1}{2}(B_1 + G^T)^T \\ \frac{1}{2}(B_1 + G^T) & \gamma\tilde{A}_\omega^{(s)} + B_2^{(s)} \end{bmatrix}$$

where

$$B_1 = -G^{-1}(A_d - A)A_d, \quad B_2 = -G^{-1}(A_d - A)G, \quad B_2^{(s)} = \frac{1}{2}(B_2 + B_2^T).$$

From the definiteness properties of the generic matrix M in Eq. (63) we know that $\tilde{A}_{\text{NDI}}^{(s)}$ is negative definite if both

$$\gamma\tilde{A}_\omega^{(s)} + B_2^{(s)} \tag{65}$$

and

$$A_d^{(s)} - \frac{1}{4}(B_1 + G^T)^T \left(\gamma\tilde{A}_\omega^{(s)} + B_2^{(s)}\right)^{-1} (B_1 + G^T) \tag{66}$$

are negative definite. Clearly, the spectrum of $\gamma\tilde{A}_\omega^{(s)} + B_2^{(s)}$ can be placed arbitrarily far out to the left on the real line by making γ large. Thus, by making γ sufficiently large we can make the matrix in Eq. (65) negative definite and shift the spectrum of the matrix

$$\frac{1}{4}(B_1 + G^T)^T \left(\gamma\tilde{A}_\omega^{(s)} + B_2^{(s)}\right)^{-1} (B_1 + G^T)$$

arbitrarily close to zero so that the matrix in Eq. (66) becomes negative definite by the properties of $A_d^{(s)}$. Then, by the estimate in Eq. (64) it follows that $\tilde{A}_{\text{NDI}}$ will be Hurwitz.

Acknowledgments

Part of this work was performed within the 'Future High-Altitude High-Speed Transport 20XX' project investigating high-speed transport, coordinated by ESA-ESTEC, and supported by the EU within the 7th Framework Programme Theme7 Transport, Contract no.: ACP8-GA-2009-2338216. Further information on FAST20XX can be found on `http://www.esa.int/fast20xx` .

References

[1]Enns, D., Bugajski, D., Hendrick, R., and Stein, G., "Dynamic Inversion: An Evolving Methodology for Flight Control Designs," *Intl. J. Control*, Vol. 59, No. 1, 1994, pp. 71–91.

[2]Lane, S. and Stengel, R., "Flight Control Design Using Non-Linear Inverse Dynamics," *Automatica*, Vol. 24, No. 4, 1988, pp. 471–483.

[3]Steinberg, M. and Page, A., "Nonlinear Adaptive Flight Control with Genetic Algorithm Design Optimization," *Intl. J. Robust and Nonlinear Control*, Vol. 9, 1999, pp. 1097–1115.

[4]Snell, S., Enns, D., and Garrard, W., "Nonlinear Inversion Flight Control for a Supermaneuverable Aircraft," *Proc. AIAA Guidance, Navigation and Control Conference*, Portland, OR, Aug 1990, AIAA paper 1990-3406.

[5]Reiner, J., Balas, G., and Garrard, W., "Flight Control Design Using Robust Dynamic Inversion and Time Scale Separation," *Automatica*, Vol. 32, No. 11, 1996, pp. 1493–1504.

[6]Enns, D., "Robustness of Dynamic Inversion VS. μ Synthesis: Lateral-Directional Flight Control Example," *Proc. AIAA Guidance, Navigation and Control Conference*, Portland, OR, Aug 1990, AIAA paper 1990-3338.

[7]Balas, G., Garrard, W., and Reiner, J., "Robust Dynamic Inversion Control Laws for Aircraft Control," *Proc. AIAA Guidance, Navigation and Control Conference*, Hilton Head Island, SC, Aug 1992, AIAA paper 1992-4329.

[8]Snell, S., "Preliminary Assessment of The Robustness of Dynamic Inversion Based Flight Control Laws," *Proc. AIAA Guidance, Navigation and Control Conference*, Hilton Head Island, SC, Aug 1992, AIAA paper 1992-4330.

[9]Qu, Z., *Robust Control Of Nonlinear Uncertain Systems*, Wiley, New York, NY, 1998.

[10]Stevens, B. L. and Lewis, F. L., *Aircraft Control and Simulation*, John Wiley & Sons, Inc., 2nd ed., 2003.

[11]Thunberg, J. and Robinson, J. W., "Block Backstepping, NDI and Related Cascade Designs for Efficient Development of Nonlinear Flight Control Laws," *Proc. AIAA Guidance, Navigation and Control Conference*, Honolulu, HI, Aug 2008, AIAA paper 2008-6960.

[12]Skjetne, R. and Fossen, T., "On Integral Control In Backstepping: Analysis of DIfferent Techniques," *Proc. American Control Conference*, Boston, MA, 2004, pp. 1899–1904.

[13]Robinson, J. W., "Block Backstepping For Nonlinear Flight Control Law Design," *Nonlinear Analysis and Synthesis Techniques for Aircraft Control*, edited by D. Bates and M. Hagström, Vol. 365 of *Lecture Notes in Control and Information Sciences Series*, Springer, Berlin, 2007, pp. 231–257.

[14]Krstić, M., Kanellakopoulos, I., and Kokotovic, P., *Nonlinear and Adaptive Control Design*, Wiley, 1995.

[15]Khalil, H., *Nonlinear Systems*, Prentice Hall, Upper Saddle River, NJ, 3rd ed., 2002.

[16]Schumacher, C., Khargonekar, P., and McClamroch, N., "Stability Analysis of Dynamic Inversion Controllers Using Time-Scale Separation," *Proc. AIAA Guidance, Navigation, and Control Conference and Exhibit*, Boston, MA, August 10-12 1998, AIAA paper 1998-4322.

[17]Zhou, K. and Doyle, J., *Essentials of Robust Control*, Prentice Hall, Upper Saddle River, NJ, 1998.

[18]"Flying Qualitites of Piloted Aircraft," US Department of Defense, December 1997, Handbook MIL-HDBK-1797 (superseding MIL-STD-1797A).

[19]Horn, R. and Johnson, C., *Topics in Matrix Analysis*, Univ. Cambridge Press, new York, NY, 1991.

View publication stats